High-resolution digital holography with the aid of coherent diffraction imaging

Zhilong Jiang,[1] Suhas P. Veetil,[2] Jun Cheng,[1] Cheng Liu,[1,*] Ling Wang,[3] and Jianqiang Zhu[1]

[1]*Shanghai Institute of Optics and Fine Mechanics, Chinese Academy of Sciences, Shanghai 201800, China*
[2]*Department of Engineering Technology and Science, Higher Colleges of Technology, Fujairah 4114, United Arab Emirates*
[3]*Department of Physics and Astronomy, KU Leuven, 3001, Heverlee, Belgium*
[*]*cheng.liu@hotmail.co.uk*

Abstract: The image reconstructed in ordinary digital holography was unable to bring out desired resolution in comparison to photographic materials; thus making it less preferable for many interesting applications. A method is proposed to enhance the resolution of digital holography in all directions by placing a random phase plate between the specimen and the electronic camera and then using an iterative approach to do the reconstruction. With this method, the resolution is improved remarkably in comparison to ordinary digital holography. Theoretical analysis is supported by numerical simulation. The feasibility of the method is also studied experimentally.

OCIS codes: (090.1995) Digital holography; (100.6640) Superresolution; (090.1970) Diffractive optics; (110.3010) Image reconstruction techniques.

References and links

1. X. Yu, M. Cross, C. Liu, D. C. Clark, D. T. Haynie, and M. K. Kim, "Measurement of the traction force of biological cells by digital holography," Biomed. Opt. Express **3**(1), 153–159 (2012).
2. M. Schnell, P. S. Carney, and R. Hillenbrand, "Synthetic optical holography for rapid nanoimaging," Nat. Commun. **5**, 3499 (2014).
3. L. Xu, X. Peng, J. Miao, and A. K. Asundi, "Studies of digital microscopic holography with applications to microstructure testing," Appl. Opt. **40**(28), 5046–5051 (2001).
4. P. Ferraro, S. Grilli, D. Alfieri, S. De Nicola, A. Finizio, G. Pierattini, B. Javidi, G. Coppola, and V. Striano, "Extended focused image in microscopy by digital Holography," Opt. Express **13**(18), 6738–6749 (2005).
5. F. Dubois, N. Callens, C. Yourassowsky, M. Hoyos, P. Kurowski, and O. Monnom, "Digital holographic microscopy with reduced spatial coherence for three-dimensional particle flow analysis," Appl. Opt. **45**(5), 864–871 (2006).
6. Y. Park, G. Popescu, K. Badizadegan, R. R. Dasari, and M. S. Feld, "Fresnel particle tracing in three dimensions using diffraction phase microscopy," Opt. Lett. **32**(7), 811–813 (2007).
7. M. Locatelli, E. Pugliese, M. Paturzo, V. Bianco, A. Finizio, A. Pelagotti, P. Poggi, L. Miccio, R. Meucci, and P. Ferraro, "Imaging live humans through smoke and flames using far-infrared digital holography," Opt. Express **21**(5), 5379–5390 (2013).
8. V. Mico, Z. Zalevsky, P. García-Martínez, and J. García, "Superresolved imaging in digital holography by superposition of tilted wavefronts," Appl. Opt. **45**(5), 822–828 (2006).
9. J. H. Massig, "Digital off-axis holography with a synthetic aperture," Opt. Lett. **27**(24), 2179–2181 (2002).
10. S. A. Alexandrov, T. R. Hillman, T. Gutzler, and D. D. Sampson, "Synthetic aperture Fourier holographic optical microscopy," Phys. Rev. Lett. **97**(16), 168102 (2006).
11. J. Ma, C. Yuan, G. Situ, G. Pedrini, and W. Osten, "Resolution enhancement in digital holographic microscopy with structured illumination," Chin. Opt. Lett. **11**(9), 090901 (2013).
12. C. Liu, Z. Liu, F. Bo, Y. Wang, and J. Zhu, "Super-resolution digital holographic imaging method," Appl. Phys. Lett. **81**(17), 3143–3145 (2002).
13. M. Paturzo and P. Ferraro, "Correct self-assembling of spatial frequencies in super-resolution synthetic aperture digital holography," Opt. Lett. **34**(23), 3650–3652 (2009).
14. J. R. Fienup, "Reconstruction of an object from the modulus of its Fourier transform," Opt. Lett. **3**(1), 27–29 (1978).
15. J. R. Fienup and C. C. Wackerman, "Phase retrieval stagnation problems and solutions," J. Opt. Soc. Am. A **3**(11), 1897–1907 (1986).

#239864 Received 29 Apr 2015; revised 16 Jul 2015; accepted 20 Jul 2015; published 3 Aug 2015

16. J. C. H. Spence, U. Weierstall, and M. Howells, "Coherence and sampling requirements for diffractive imaging," Ultramicroscopy **101**(2-4), 149–152 (2004).
17. U. Weierstall, Q. Chen, J. C. H. Spence, M. R. Howells, M. Isaacson, and R. R. Panepucci, "Image reconstruction from electron and X-ray diffraction patterns using iterative algorithms: experiment and simulation," Ultramicroscopy **90**(2-3), 171–195 (2002).
18. R. W. Gercherg, "A practical algorithm for the determination of phase from image and diffraction plane pictures," Optik (Stuttg.) **35**, 237–246 (1972).
19. G. Zheng, R. Horstmeyer, and C. Yang, "Wide-field, high-resolution Fourier ptychographic microscopy," Nat. Photonics **7**(9), 739–745 (2013).
20. H. M. L. Faulkner and J. M. Rodenburg, "Movable aperture lensless transmission microscopy: a novel phase retrieval algorithm," Phys. Rev. Lett. **93**(2), 023903 (2004).
21. J. M. Rodenburg and H. M. L. Faulkner, "A phase retrieval algorithm for shifting illumination," Appl. Phys. Lett. **85**(20), 4795–4797 (2004).
22. A. M. Maiden and J. M. Rodenburg, "An improved ptychographical phase retrieval algorithm for diffractive imaging," Ultramicroscopy **109**(10), 1256–1262 (2009).
23. F. Zhang, I. Peterson, J. Vila-Comamala, A. Diaz, F. Berenguer, R. Bean, B. Chen, A. Menzel, I. K. Robinson, and J. M. Rodenburg, "Translation position determination in ptychographic coherent diffraction imaging," Opt. Express **21**(11), 13592–13606 (2013).

1. Introduction

Digital holography has developed rapidly in recent years for its distinct advantages over traditional holography including higher imaging speed and lower requirement on the setup stability. This has found many applications in the field of microscopy [1,2], three dimensional imaging [3,4], particle tracing [5,6] and monitoring [7] recently. However, in most cases, the holograms of digital holography were recorded with an electronic camera (generally a CCD camera) and the reconstructed resolution is lower than that of photographic materials by at least an order of magnitude [8]. This is a serious limitation and thus making digital holography less preferable for many interesting applications.

Various approaches were taken in the recent past to increase the spatial resolution of digital holography to achieve so called super-resolution. An effective way is to increase the numerical aperture (NA) of the holographic system. A synthetic aperture method was proposed to achieve it by recording section-holograms at different positions and later combining these into a composite hologram [9]. The NA of the holographic system can also be increased by rotating the specimen while recording a set of Fourier holograms [8,10] or by using structured illumination [11]. In all these methods, higher frequency components of object waves which are originally off the CCD target are made to diffract into the CCD and thus achieving a spatial resolution which is higher than that of original digital holography under the diffraction limit. A grating placed between the specimen and CCD can also be used to achieve a higher resolution, wider field of view, and reduced scattering noise [12,13]. However, in this method, the grating used need to be dustless and the reconstructed image contains many images of different diffraction order and only the resolution of zero order image is enhanced. Moreover, an overlapping of these reconstructed images may happen if the specimen size isn't small enough, and the resolution can only be enhanced in the direction vertical to the grating grooves.

In this paper, we suggested another method to achieve a higher resolution digital holographic imaging. A phase plate with a random phase in place of a grating can effectively scatter off high-frequency components into the CCD target, and hence it can be used to improve the resolution of digital holography in all directions along with an iterative algorithm for reconstruction. To effectively retrieve more off high-frequency components of object waves which are usually scattered off the CCD target area, a tiny hole with sharp edge is used as a spatial constraint on the object plane, and a complex amplitude constraint is used on the recording plane. The feasibility of the method is tested experimentally, and the spatial resolution of the reconstructed image was improved by a factor of two compared to original digital holography.

#239864 Received 29 Apr 2015; revised 16 Jul 2015; accepted 20 Jul 2015; published 3 Aug 2015

2. Basic principle of the suggested method

The schematic of the suggested method is shown in Fig. 1. A fixed specimen is illuminated with a collimated planar laser beam. The transmitted light through a pinhole is scattered by a random phase plate before forming a diffraction pattern O on the CCD target. This diffraction pattern interferes with a reference wave R and forms an off-axis hologram with the intensity I

$$I = |O|^2 + |R|^2 + OR^* + O^*R \tag{1}$$

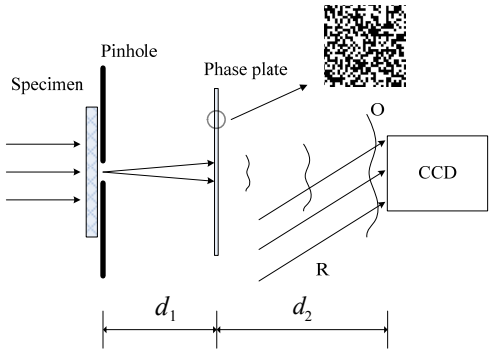

Fig. 1. Schematic of the suggested method.

According to the principle of Fourier Optics, the distribution of the random phase plate $\tilde{t}(x, y)$ can be rewritten as

$$\tilde{t}(x, y) = \iint \tilde{t}(f_x, f_y) e^{-i2\pi(f_x x + f_y y)} df_x df_y \tag{2}$$

where $e^{-i2\pi(f_x x + f_y y)}$ can be considered as a sinusoidal grating with a period of $1/\sqrt{(f_x^2 + f_y^2)}$ in the direction of ($f_x / \sqrt{(f_x^2 + f_y^2)}$, $f_y / \sqrt{(f_x^2 + f_y^2)}$). Equation (2) indicates that a random phase plate can be regarded as a collection of gratings with different periods and directions, thus more high-frequency components of the object waves can be scattered into the CCD as compared to a regular grating, which has the fixed period and orientation. For clarity, the ray diagrams of the object waves are shown in Fig. 2 and only a point object P is discussed for simplicity. Figure 2(a) shows the ray diagram in traditional holography, where all the object waves freely propagate to the recording plane, and only the central wave reaches the CCD target and is digitally recorded. Because of the limited size of the CCD, only a smaller portion of the total object waves were recorded. Figure 2(b) shows the ray diagram when a grating is placed between the CCD and the specimen. The object waves in the central column are recorded due to the diffraction from the grating, and accordingly the resolution can be enhanced in the vertical direction. Figure 2(c) shows the diffraction situation when a random phase plate is applied. All the object waves are scattered uniformly into the CCD area in this case and hence a better resolution is obtained in various directions. The resolution of digital holography can reach a threefold enhancement with a regular grating [13], and since the random phase plate is composed of gratings of different periods and directions, in theory, a threefold enhancement in resolution regardless of direction can be achieved with a random phase plate.

#239864 Received 29 Apr 2015; revised 16 Jul 2015; accepted 20 Jul 2015; published 3 Aug 2015

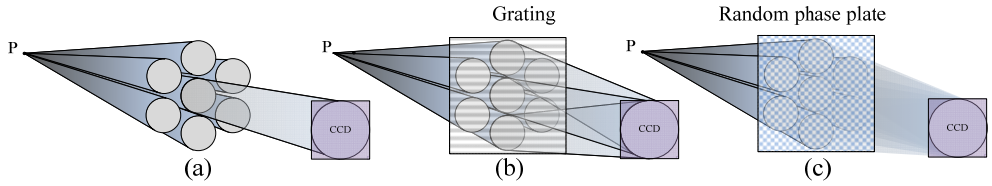

Fig. 2. Ray diagrams of the object wave: (a) without a grating or a random phase plate in the setup. (b) with a grating used in the setup. (c) with a random phase plate used in the setup.

Though Fig. 2(b) and Fig. 2(c) may seem almost identical in the first glance, except in the respective transmission functions, the reconstruction algorithms needed are fundamentally different. When a grating is used, the resolution-enhanced image can be explicitly reconstructed by back-propagating the light field from the hologram plane to the object plane via the grating plane. In the reconstruction process, a series of images of different orders were generated, and the interval between these images corresponds to the period of grating. If the same reconstruction algorithm is used in the case of random phase plate, an overlap of countless images would occur and no clear images would be generated. Hence a different iterative algorithm for reconstruction is suggested while using a random phase plate. This iterative algorithm is much similar to that of coherent diffraction imaging [14–18]. The iteration is as follows:

(1) The complex amplitude of the diffraction pattern $diff_{ccd}$ can be obtained by the standard off-axis digital holography and then to be placed into a large zero matrix to form a new matrix $Diff_{ccd}$. The region of $diff_{ccd}$ in the new matrix is defined as S_{ccd}. Then the iteration starts with a guessed object function O_0.

(2) Apply the spatial constraint on the object plane,

$$O_{n+1} = O_n^{'} \cdot S_{hole} + (O_n - \alpha O_n^{'}) \cdot (1 - S_{hole}) \tag{3}$$

where O_n and $O_n^{'}$ are the current and the updated estimate of the object function in the n^{th} (n = 0,1,2,...) iteration, α is a constant feedback parameter and takes value in the range of [0.5, 1], and S_{hole} has a value of one inside the pinhole and a value of zero outside, it is used as the spatial constraint on the object plane in the iterative computation.

(3) Propagate O_{n+1} to the random phase plate plane and then multiply with the modulation function of the random phase plate to get the transmitted filed Ψ_{n+1},

$$\Psi_{n+1} = \psi_{n+1} \cdot t \tag{4}$$

where ψ_{n+1} is the diffraction pattern of the random phase plate plane and t is the transmission function of the random phase plate.

(4) Propagate the transmitted field Ψ_{n+1} to the recording plane to get a new complex diffraction pattern $Diff_{n+1}$.

(5) Apply the intensity constraint on the recording plane. The central part of the diffraction pattern $Diff_{n+1}$ were assigned to the original value of $diff_{ccd}$ and keep the values of other area unchanged to get an updated diffraction pattern $Diff_{n+1}^{'}$.

#239864 Received 29 Apr 2015; revised 16 Jul 2015; accepted 20 Jul 2015; published 3 Aug 2015

(6) To eliminate the noise caused by the Fourier repeats, a couple of pixels at the edge of diffraction pattern $Diff'_{n+1}$ are forced to be zero, then a revised diffraction pattern $Diff'_{n+1}$ is obtained.

(7) Back-propagate the new $Diff'_{n+1}$ to the object plane via the phase plate plane to get the updated object function O'_{n+1}. On the random phase plate plane, the following formula which is similar to the Wigner-filter is used to remove the modulation of light beam caused by the random phase plate.

$$\psi'_{n+1} = \psi_{n+1} + \frac{|t|}{|t_{\max}|} \frac{t^*}{(|t|^2 + \beta)} \cdot (\Psi'_{n+1} - \Psi_{n+1}) \tag{5}$$

where Ψ'_{n+1} is the updated transmitted field and ψ'_{n+1} is the updated diffraction pattern on the random phase plate plane. β is a constant parameter used to prevent a divide-by-zero situation occurring if $|t| = 0$.

(8) Evaluate the quality of the reconstructed O'_{n+1}. If it meets the requirement, the calculation stops, else the calculation goes on from step (2) to step (7).

The above iterative algorithm is essentially a combination of the modified Hybrid-Input-Out (HIO) algorithm and the digital holography. HIO algorithm was developed by Fienup from the Gerchberg-Saxton (G-S) algorithm [18]. While G-S algorithm uses two frames of diffraction intensity as the intensity constraint on two planes with a proper interval along the optical axis, HIO algorithm uses one frame of diffraction intensity as the intensity constraint on the recording plane and a pinhole as the spatial constraint on the object plane. Different from the traditional HIO algorithm, the suggested algorithm uses the reconstruction of the digital holography as the complex constraints on the recording plane in place of the intensity constraint, and what retrieved is the diffraction beyond the CCD chip that cannot be recorded in the common digital holography. In comparison with the Fourier ptychographic microscopy (FPM) [19], which needs to do a raster scanning on the object and record hundreds of diffraction patterns, the suggested method only records one frame of hologram and one frame of diffraction intensity, so it is a very speedy high resolution phase imaging method.

3. Numerical simulation

The feasibility of the suggested method is verified by numerical simulations on recording and reconstructing procedures.

The assumed modulus and phase distributions of the specimen used in simulation are shown in Fig. 3(a) and Fig. 3(b), respectively. The red circles indicate the pinhole with a diameter of 1.2 mm, which is used as the spatial constraint in the iterative computation. A collimated beam with the wavelength of 632.8 nm is used as an illumination. The CCD is assumed to be 512 × 512 pixel with a pixel size of 7.4 × 7.4 μm^2. The random phase plate has a structure shown in Fig. 1, where the dark and bright areas indicate phase jumps of 0 and π respectively. Since the plate is a binary pseudo random phase object, and only when a large number of its pixels are illuminated the light incident on it can be fully scattered. This means its distance to the objet should be large enough to form a speckle field behind it. The d_2 in Fig. 1 should be large enough to get a fully developed speckle patterns, else no clear interference fringe can be obtained. The distances d1 and d2 should be decided according to the structure of the phase plate and the pixel size of the CCD. In the simulations they are 50 mm and 100 mm, respectively.

#239864 Received 29 Apr 2015; revised 16 Jul 2015; accepted 20 Jul 2015; published 3 Aug 2015

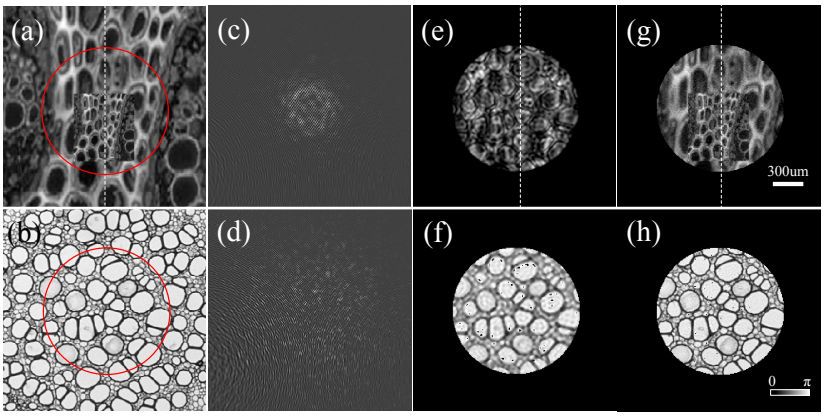

Fig. 3. (a) and (b) are the assumed modulus and phase images of the specimen, respectively. (c) Hologram obtained with common digital holography. (d) Hologram of the suggested method. (e) and (f) are the reconstructed modulus and phase images in common digital holography, respectively. (g) and (h) are the reconstructed modulus and phase images with the suggested method, respectively.

Figure 3(c) shows the recorded hologram in common digital holography and Fig. 3(d) is the hologram obtained with our suggested method. One can easily make out the difference between these two holograms. Figure 3(e) and Fig. 3(f) show the reconstructed modulus and phase images of the specimen in common digital holography, where the details of the specimen could be barely identified. This was due to loss of high-frequency components. Figure 3(g) and Fig. 3(h) show the reconstructed modulus and phase images with the suggested method after 1000 iterations. The resolution has improved significantly with our method in comparison to images obtained by direct holographic reconstruction in Fig. 3(e) and Fig. 3(f).

For further comparison, the modulus in different situations were taken along the white dashed lines in Fig. 3(a), Fig. 3(e) and Fig. 3(g) are shown in Fig. 4(a), and indicated by blue, green and red line profile respectively. The blue line diverges from the green one but overlaps quite well with the red one, thus resulting in a higher resolution in Fig. 3(g). In fact, the smallest discernible cells in the modulus image of Fig. 3(e) is 66.6 μm in size and is 22.2 μm in that of Fig. 3(g), which means the resolution of the reconstructed image has been enhanced by threefold with the suggested method. Figure 4(b) shows the modulus of the initial diffraction pattern on the recording plane, where the rectangle in dashed line indicates the edge of the CCD target. Figure 4(c) shows the modulus of the reconstructed diffraction pattern after 1000 iterations with the suggested method. Retrieving high-frequency components in iterations provides a better resolution over conventional methods.

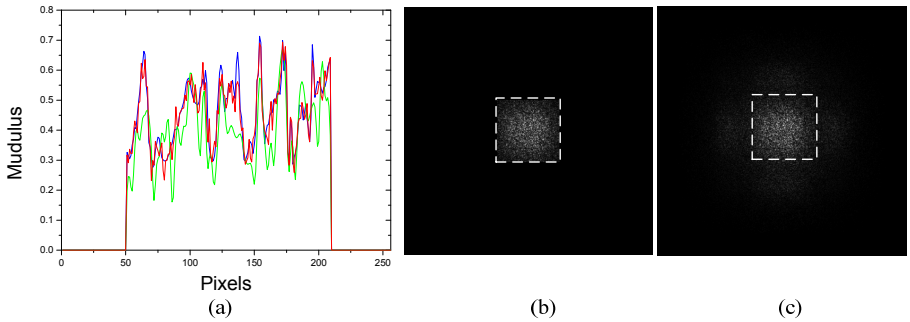

Fig. 4. (a) The line profiles of modulus along white dashed lines in Fig. 3(a), Fig. 3(e) and Fig. 3(g) and are indicated by blue, green and red line respectively. (b) The initial diffraction pattern on the recording plane. (c) The reconstructed diffraction pattern after 1000 iterations with the suggested method.

#239864 Received 29 Apr 2015; revised 16 Jul 2015; accepted 20 Jul 2015; published 3 Aug 2015

To evaluate the performance of the suggested method quantitatively, the following formulas are adopted to calculate the reconstruction error,

$$E_0(n) = \frac{\sum_r |O(r) - \gamma O_n(r)|^2}{\sum_r |O(r)|^2} \tag{6}$$

$$\gamma = \frac{\sum_r O(r) O_n^*(r)}{\sum_r |O_n(r)|^2} \tag{7}$$

where $O_n(r)$ is the reconstructed object distribution after n iterations with the suggested method. Parameter γ allows a constant offset in both modulus and phase of the object between true and reconstructed ones. Figure 5(a) shows the evaluation of the reconstruction error. In our suggested method, where the reconstruction error decreases rapidly with increase in the number of iterations, the reconstruction error becomes smaller than 0.02 after 400 iterations, which is 7.5 times smaller than the error of 0.15 obtained in common digital holography; thus leading to a well converging result.

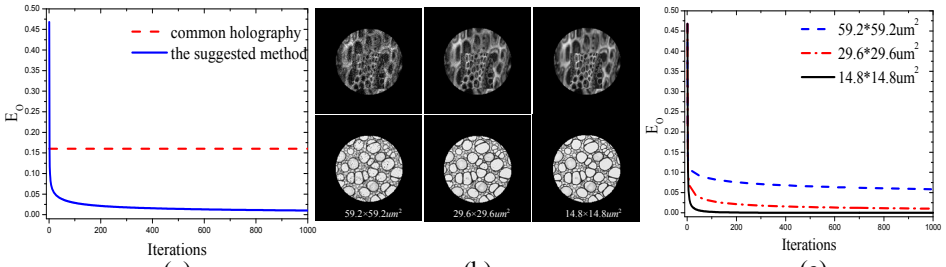

(a) (b) (c)

Fig. 5. (a) The evaluation of the reconstruction error. (b) The reconstructed modulus and phase with three random phase plates of different pixel size of 59.2 × 59.2 μm^2, 29.6 × 29.6 μm^2 and 14.8 × 14.8 μm^2, respectively. (c) The evaluation of the reconstruction error changes with the number of iterations.

A key factor in the suggested method is the random phase plate and the influence of its parameter on the performance of iteration algorithm is evaluated. Figure 5(b) shows the reconstructed holographic results by using three different random phase plates with the pixel size of 59.2 × 59.2 μm^2, 29.6 × 29.6 μm^2 and 14.8 × 14.8 μm^2 respectively, where the resolution enhancement is inversely proportional to the pixel size of the random phase plate. For a quantitative comparison, the reconstruction errors with increase in the number of iterations are shown in Fig. 5(c), where a pixel size of 14.8 × 14.8 μm^2 shows a faster convergence and a lower reconstruction error. This means that a smaller pixel size of the random phase plate can effectively diffract more high-frequency components into the detector sensor and thus resulting in a high resolution in the reconstructed holographic images.

4. Experiment and result

The experimental setup for the suggested method is shown in Fig. 6. A specimen of a fixed USAF resolution target is used to demonstrate the validity of the suggested method. A collimated laser beam with the wavelength of 632.8 nm is divided into two sets of beams with a beam splitter, one forms a reference wave after passing through a spatial filter and a collimating lens, while the other forms an object wave with a dispersed spherical wave-front after modulated by a pinhole and a random phase plate. The hologram is recorded with a CCD with

#239864 Received 29 Apr 2015; revised 16 Jul 2015; accepted 20 Jul 2015; published 3 Aug 2015

512 × 512 pixels with a pixel size of 7.4 × 7.4 μm^2 . The pinhole used is 1 mm in diameter and is kept at a distance of 60.7 mm from the random phase plate. The distance from the random phase plate to the CCD is 90.4 mm.

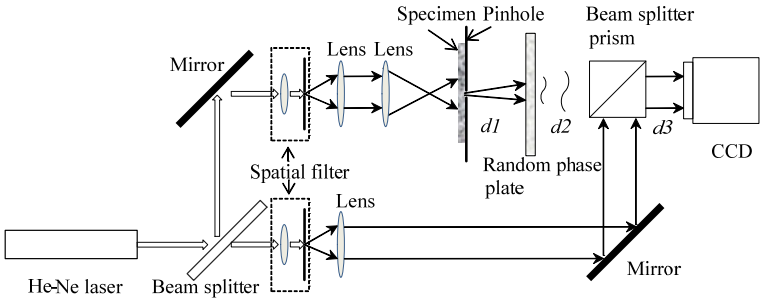

Fig. 6. The experimental setup. The focal length of the lens is 100 mm and the beam splitter prism used is 25.4 mm in width. d_1 is the distance between the pinhole and the random phase plate; d_2 is the distance between the random phase plate and the beam splitter prism; d_3 is the distance between the beam splitter prism and the CCD. *d1* = 60.7mm, *d2* = 44.5mm, *d3* = 20.5mm.

The phase of the random phase plate has a value from 0 to π, chosen randomly with the pixel size of 14.8 × 14.8 μm^2, and its phase distribution can be measured accurately through Ptychographic Iterative Engine (PIE) [20–23] experiment. The same experimental setup in Fig. 6 can be used as a PIE setup and the experimentally measured modulus and phase information of the random phase plate are shown in Fig. 7.

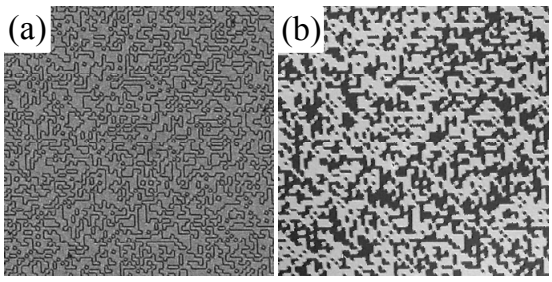

Fig. 7. The modulus (a) and the phase (b) distribution of the random phase plate measured through the PIE experiment.

The measured modulus and phase distribution of the random phase plate remain unchanged if the illumination remains stable. Several holographic data are recorded in this resolution-enhanced holography experiment. For a comparison, ordinary holographic recording is also done on the same setup by removing the random phase plate. Figure 8(a) shows the hologram recorded in ordinary holography. The reconstructed modulus and phase images of the USAF resolution target are shown in Fig. 8(b) and Fig. 8(c), respectively. Only a blurred image is reconstructed as shown in Fig. 8(b), and the resolution achieved is about 27.8 μm (17.96 LP/mm) as shown in the zoomed in image. Figure 8(d) shows the hologram obtained with the suggested holography experiment. The reconstructed holography results with the suggested iterative algorithm shown in Fig. 8(e) and Fig. 8(f) are the modulus and phase images, respectively. The resolution achieved is about 13.9 μm (36 LP/mm). That is, a twofold increase in resolution is obtained with the setup. Since the phase plate is a binary pseudo random phase plate, some of the light scattered by its sharp edges between 'π' and '0' cannot be retrieved correctly due to their low energy and the limited sensitivity of the CCD, and then

#239864 Received 29 Apr 2015; revised 16 Jul 2015; accepted 20 Jul 2015; published 3 Aug 2015

weak speckles will be generated in final reconstruction, which can be found in Fig. 8(e) when compared to Fig. 8(b).

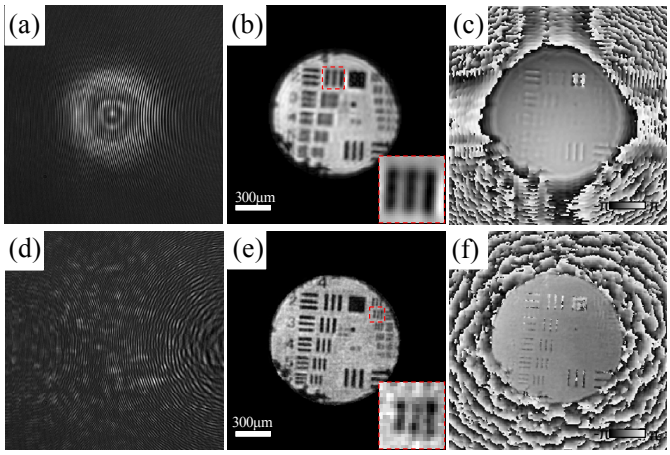

Fig. 8. (a) The hologram in ordinary holography experiment. (b) and (c) are the reconstructed modulus and phase in ordinary holography experiment, respectively. (d) The hologram in the suggested holography experiment. (e) and (f) are the reconstructed modulus and phase in the suggested holography experiment, respectively.

Another experiment is also done to image a biological specimen of the pumpkin stem with the suggested method. Figure 9(a) shows the hologram of an ordinary holography, and the reconstructed modulus and phase images are shown in Fig. 9(b) and Fig. 9(c), respectively. Only a blurred image is reconstructed as shown in Fig. 9(b) and the cell structure of the specimen can be hardly seen. Figure 9(d) shows the hologram obtained with the suggested method, and the reconstructed modulus and the phase image are shown in Fig. 9(e) and Fig. 9(f) respectively. The structure of individual cell is quite clear. This result supports the theoretical analysis well.

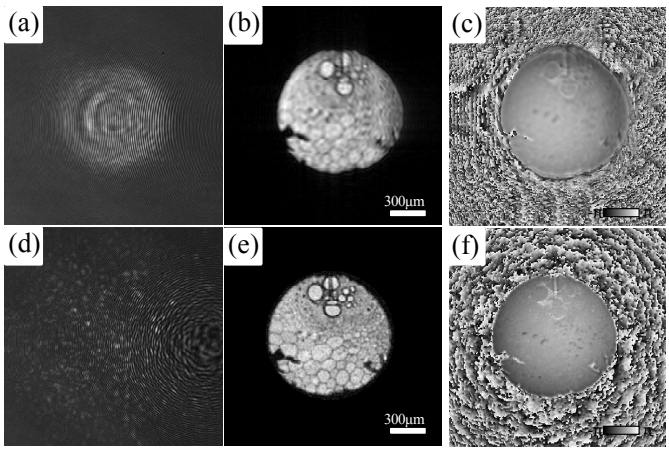

Fig. 9. Digital holography results with a biological specimen of pumpkin stem. (a) The hologram in ordinary holography experiment. (b) and (c) are the reconstructed modulus and phase in ordinary holography experiment, respectively. (d) The hologram in the suggested holography experiment. (e) and (f) are the reconstructed modulus and phase in the suggested holography experiment, respectively.

#239864 Received 29 Apr 2015; revised 16 Jul 2015; accepted 20 Jul 2015; published 3 Aug 2015

5. Conclusion

The new approach outlined in this paper using a random phase plate in holographic recording setup and a modified iterative algorithm in the reconstruction provides a significant improvement in the achievable resolution in digital holography. The feasibility of the suggested method is demonstrated in numerical simulation and experiment. The method is simple in its setup and the experimental procedures are easy to implement and would be an excellent solution to the problem of low resolution in the digital holographic microscopy.

Acknowledgments

This research is supported by One Hundred Person Project of the Chinese Academy of Sciences under Grant No.902012312D1100101 and Project of the Chinese Academy of Sciences under Grant 29201431151100301.

#239864 Received 29 Apr 2015; revised 16 Jul 2015; accepted 20 Jul 2015; published 3 Aug 2015